

Photochemistry of the Clusters $\text{Os}_3(\text{CO})_{10}(\text{L})$ ($\text{L} = 2,2'$ -Bipyridine, $2,2'$ -Bipyrimidine, $2,3$ -Dipyrid-2-ylpyrazine, $2,3$ -Dipyrid-2-ylbenzoquinoxaline). Reversible Opening of an Os–Os Bond with Formation of a Zwitterion

J. W. M. van Outersterp, M. T. Garriga Oostenbrink, H. A. Nieuwenhuis, D. J. Stufkens,* and F. Hartl

Anorganisch Chemisch Laboratorium, Universiteit van Amsterdam, J. H. van't Hoff Research Institute, Nieuwe Achtergracht 166, 1018 WV Amsterdam, The Netherlands

Received November 17, 1994[Ⓢ]

The complexes $\text{Os}_3(\text{CO})_{10}(\text{L})$ ($\text{L} = 2,2'$ -bipyridine (bpy), $2,2'$ -bipyrimidine (bpym), $2,3$ -dipyrid-2-ylpyrazine (dpp), and $2,3$ -dipyrid-2-ylbenzoquinoxaline (dpb)) were synthesized, and their low-energy $\text{Os} \rightarrow \text{L}$ (MLCT) transitions were characterized with resonance Raman spectroscopy. Continuous wave excitation into the MLCT transitions does not lead to product formation. However, rapid-scan IR and nano- and picosecond time-resolved absorption spectra show the formation of a transient species (for $\text{L} = \text{bpy}$, bpym , and dpp) which reacts back to give the parent complex. In toluene the transient has a lifetime of less than 10 ns and is assigned to an MLCT state of the cluster. In coordinating solvents a different transient species is observed with a lifetime that strongly depends on the coordinating ability of the solvent and the basic properties of L (200–900 ns in tetrahydrofuran (THF), 5–20 s in CH_3CN). The transient species could even be obtained as a stable photoproduct by reaction in 2-MeTHF at 133 K and upon irradiation at room temperature in the presence of a halide salt. The transient species is proposed to be the zwitterion $\text{Os}^-(\text{CO})_4-\text{Os}(\text{CO})_4-\text{Os}^+(\text{CO})_2(\text{S})(\text{L})$. The positive charge of the metal in the $\text{Os}^+(\text{CO})_2(\text{S})(\text{L})$ moiety is evident from the Raman and $^1\text{H-NMR}$ spectra, the coordination of the solvent from its large influence on the lifetime, and the absorption maximum of the transient intermediate. Since the zwitterion is already formed within 50 ps after the laser pulse, it is most probably produced by reaction from the MLCT state(s). A coordinating solvent molecule may initiate this reaction by coordination to the metal center of the $\text{Os}(\text{CO})_2(\alpha\text{-diimine})$ fragment in its MLCT state. The extra negative charge donated by the solvent may then cause a heterolytic splitting of an Os–Os bond with formation of the zwitterion.

Introduction

Metal–metal bonded complexes such as $\text{M}_2(\text{CO})_{10}$ ($\text{M} = \text{Mn}$, Re), $\text{Cp}_2\text{Fe}_2(\text{CO})_4$ ($\text{Cp} = \text{cyclopentadiene}$), and $\text{Cp}_2\text{M}_2(\text{CO})_6$ ($\text{M} = \text{Mo}$, W) undergo both metal–metal bond homolysis and release of CO as primary photoprocesses.^{1–4} The homolysis reaction results in the formation of radicals; the CO-loss reaction produces carbonyl bridged species such as $\text{Mn}_2(\text{CO})_9$.^{5,6} The clusters $\text{M}_3(\text{CO})_{12}$ ($\text{M} = \text{Ru}$, Os) undergo the same primary photoprocesses, but their photoproducts differ from those of the dinuclear complexes. Thus, the homolysis reaction does not produce a diradical species but instead an isomer of $\text{M}_3(\text{CO})_{12}$ possessing a bridging carbonyl ligand.^{7–14} Recently, we have

investigated in detail the photochemistry of a series of related complexes $\text{L}_n\text{M}'\text{M}(\text{CO})_3(\alpha\text{-diimine})$ ($\text{L}_n\text{M}' = (\text{CO})_5\text{Mn}$, $(\text{CO})_5\text{Re}$, $(\text{CO})_4\text{Co}$, $\text{Cp}(\text{CO})_2\text{Fe}$, Ph_3Sn ; $\text{M} = \text{Mn}$, Re ; $\alpha\text{-diimine} = \text{bpy}$, phen , etc.), which contain a metal–metal bond and show an intense $\text{M} \rightarrow \alpha\text{-diimine}$ charge-transfer (MLCT) band in the visible spectral region.^{15–22} Again, irradiation of these complexes gave rise to homolysis of the $\text{M}'\text{–M}$ bond and/or release of CO from the $\text{M}(\text{CO})_3(\alpha\text{-diimine})$ fragment. Rhenium complexes $\text{L}_n\text{M}'\text{Re}(\text{CO})_3(\alpha\text{-diimine})$ exhibited $\text{M}'\text{–Re}$ bond homolysis only, while both reactions occurred for some $\text{L}_n\text{M}'\text{Mn}(\text{CO})_3(\alpha\text{-diimine})$ complexes. Much attention has been paid to the mechanism of these homolysis reactions, which resulted in the formation of $^*\text{M}'\text{L}_n$ and $[\text{M}(\text{CO})_3(\alpha\text{-diimine})]^*$ radicals. Homolysis of the $\text{M}'\text{–M}$ bond was explained by surface crossing from the MLCT states to a reactive $\sigma\pi^*$ state, in which σ represents the metal–metal bonding orbital and π^* the lowest unoccupied orbital of the $\alpha\text{-diimine}$.²³ The presence of such a

* To whom correspondence should be addressed.

[Ⓢ] Abstract published in *Advance ACS Abstracts*, November 1, 1995.

- (1) Geoffroy, G. L.; Wrighton, M. S. *Organometallic Photochemistry*; Academic Press: New York, 1979.
- (2) Meyer, T. J.; Caspar, J. V. *Chem. Rev.* **1985**, *85*, 187.
- (3) Stiegman, A. E.; Tyler, D. R. *Coord. Chem. Rev.* **1985**, *63*, 217.
- (4) Stufkens, D. J. In *Stereochemistry of Organometallic and Inorganic Compounds*; Bernal, I., Ed.; Elsevier: Amsterdam, 1989; Vol. 3; p 226.
- (5) Hepp, A. F.; Wrighton, M. S. *J. Am. Chem. Soc.* **1983**, *105*, 5934.
- (6) Dunkin, I. R.; Härter, P.; Shields, C. J. *J. Am. Chem. Soc.* **1984**, *106*, 7248.
- (7) Bentsen, J. G.; Wrighton, M. S. *J. Am. Chem. Soc.* **1987**, *109*, 4530.
- (8) Desrosiers, M. F.; Ford, P. C. *Organometallics* **1982**, *1*, 1715.
- (9) Desrosiers, M. F.; Wink, D. A.; Ford, P. C. *Inorg. Chem.* **1985**, *24*, 1.
- (10) Desrosiers, M. F.; Wink, D. A.; Trautman, R.; Friedman, A. E.; Ford, P. C. *J. Am. Chem. Soc.* **1986**, *108*, 1917.
- (11) Ford, P. C. *J. Organomet. Chem.* **1990**, *383*, 339.
- (12) Malito, J.; Markiewicz, S.; Poë, A. *Inorg. Chem.* **1982**, *21*, 4335.
- (13) Poë, A. J.; Sekhar, C. V. *J. Am. Chem. Soc.* **1986**, *108*, 3673.
- (14) Brodie, N. M. J.; Huq, R.; Malito, J.; Markiewicz, S.; Poë, A. J.; Sekhar, V. S. *J. Chem. Soc., Dalton Trans.* **1989**, 1933.

- (15) Stufkens, D. J. *Coord. Chem. Rev.* **1990**, *104*, 39.
- (16) van Dijk, H. K.; van der Haar, J.; Stufkens, D. J.; Oskam, A. *Inorg. Chem.* **1989**, *28*, 75.
- (17) Andréa, R. R.; de Lange, W. G. J.; Stufkens, D. J.; Oskam, A. *Inorg. Chem.* **1989**, *28*, 318.
- (18) van der Graaf, T.; van Rooy, A.; Stufkens, D. J.; Oskam, A. *Inorg. Chim. Acta* **1991**, *187*, 133.
- (19) van der Graaf, T.; Stufkens, D. J.; Oskam, A.; Goubitz, K. *Inorg. Chem.* **1991**, *30*, 599.
- (20) Servaas, P. C.; Stor, G. J.; Stufkens, D. J.; Oskam, A. *Inorg. Chim. Acta* **1990**, *178*, 185.
- (21) Kokkes, M. W.; Stufkens, D. J.; Oskam, A. *Inorg. Chem.* **1985**, *24*, 2934.
- (22) Rossenaar, B. D.; van der Graaf, T.; van Eldik, R.; Langford, C. H.; Stufkens, D. J.; Vlček, A., Jr. *Inorg. Chem.* **1994**, *33*, 2865.
- (23) Stufkens, D. J. *Comments Inorg. Chem.* **1992**, *13*, 359.

reactive $\sigma\pi^*$ state is not restricted to these and other metal-metal bonded complexes. Similar homolysis reactions have been observed for the metal-alkyl bonded complexes ZnR_2 - $(\alpha\text{-diimine})$,²⁴ $\text{Re}(\text{R})(\text{CO})_3(\text{R}'\text{-DAB})$ ($\text{DAB} = 1,4\text{-diaz-1,3-butadiene}$)²⁵ and $\text{Ru}(\text{X})(\text{R})(\text{CO})_2(\alpha\text{-diimine})$ ($\text{X} = \text{halide}$)²⁶ and for a series of N,Si-chelated Ir^{III} complexes.²⁷⁻²⁹ More and more the reactive $\sigma\pi^*$ state appears to be a common property of a rather large group of complexes possessing both low-energy MLCT transitions and a covalent metal-metal or metal-alkyl bond. On the basis of the behavior of the dinuclear complexes $\text{L}_n\text{M}'\text{M}(\text{CO})_3(\alpha\text{-diimine})$, it is expected that the substituted clusters $\text{Os}_3(\text{CO})_{10}(\alpha\text{-diimine})$ will also undergo a homolytic splitting of an Os-Os bond with formation of a diradical species. Alternatively, these clusters may undergo a similar photoreaction as the unsubstituted cluster $\text{Os}_3(\text{CO})_{12}$ and form a carbonyl bridged isomer of the parent complex.

In order to establish the photochemical mechanism and characterize the primary photoproducts, we have studied in detail the photoreactions of $\text{Os}_3(\text{CO})_{10}(\alpha\text{-diimine})$ ($\alpha\text{-diimine} = 2,2'$ -bipyridine (bpy), 2,2'-bipyrimidine (bpym), 2,3-dipyrid-2-ylpyrazine (dpp), and 2,3-dipyrid-2-ylbenzoquinoline (dpb)). The structure of these clusters, derived from an X-ray structure determination of $\text{Os}_3(\text{CO})_{10}(\text{iPr-DAB})$,³⁰ is shown in Figure 1. This figure also presents the schematic structures of the $\alpha\text{-diimine}$ ligands used.

Experimental Section

Materials and Preparations. $\text{Os}_3(\text{CO})_{12}$ (Strem Chemicals), bpy (Aldrich), bpym (Johnson & Matthey), and dpp (Aldrich) were used as received. The solvents 2-MeTHF (Merck), THF (Merck), hexane (Merck), and toluene (Merck), used for the syntheses and photochemical reactions, were distilled over Na wire under a N_2 atmosphere. Acetonitrile (Janssen Chimica) was distilled from P_2O_5 prior to use.

The dpb ligand was synthesized as described previously.³¹ The $\text{Os}_3(\text{CO})_{10}(\text{L})$ complexes were prepared according to literature procedures.³⁰ $\text{Os}_3(\text{CO})_{10}(\text{bpy})$: $^1\text{H-NMR}$ (acetone- d_6): δ 9.62 (d, 2 H6), 8.93 (d, 2 H3), 8.35 (dd, 2 H5), 7.81 (dd, 2 H4). Elemental analysis of $\text{C}_{20}\text{H}_8\text{N}_2\text{O}_{10}\text{Os}_3$ found (calcd): %C = 24.04 (23.86), %H = 1.10 (0.80), %N = 2.75 (2.78). $\text{Os}_3(\text{CO})_{10}(\text{bpym})$: $^1\text{H-NMR}$ (acetone- d_6): δ 9.80 (d, 2 H6), 9.38 (d, 2 H4), 7.96 (dd, 2 H5). Elemental analysis of $\text{C}_{18}\text{H}_6\text{N}_4\text{O}_{10}\text{Os}_3$ found (calcd): %C = 21.53 (21.43), %H = 0.71 (0.60), %N = 5.41 (5.55). $\text{Os}_3(\text{CO})_{10}(\text{dpp})$: $^1\text{H-NMR}$ (acetone- d_6): δ 9.73 (d, pyz-H6 (pyz = pyridazine)), 9.51 (d, (py-H6' (py = (pyridine))), 8.77 (d, pyz-H5), 8.74 (d, py-H6), 8.27 (dd, py-H4), 8.19 (d, py-H3), 7.88 (dd, py-H4'), 7.75 (dd, py-H5), 7.66 (dd, py-H5'), 7.49 (d, py-H3'). Elemental analysis of $\text{C}_{24}\text{H}_{10}\text{N}_4\text{O}_{10}\text{Os}_3$ found (calcd): %C = 26.63 (26.57), %H = 1.06 (0.93), %N = 5.08 (5.16). $\text{Os}_3(\text{CO})_{10}(\text{dpb})$: $^1\text{H-NMR}$ (acetone- d_6): δ 9.75 (d), 9.31 (d), 8.71 (s), 8.40 (d), 8.33 (m), 7.98 (m), 7.78 (m), 7.55 (d).

Spectroscopic Measurements and Instrumentation. UV-vis absorption spectra were recorded on a Varian Cary 4E or Perkin-Elmer Lambda 5 spectrophotometer. FTIR spectra were recorded on a BioRad FTS-7 infrared spectrometer (16 scans, resolution 2 cm^{-1}). Rapid scan FTIR spectra were measured on a BioRad 60A spectrometer after

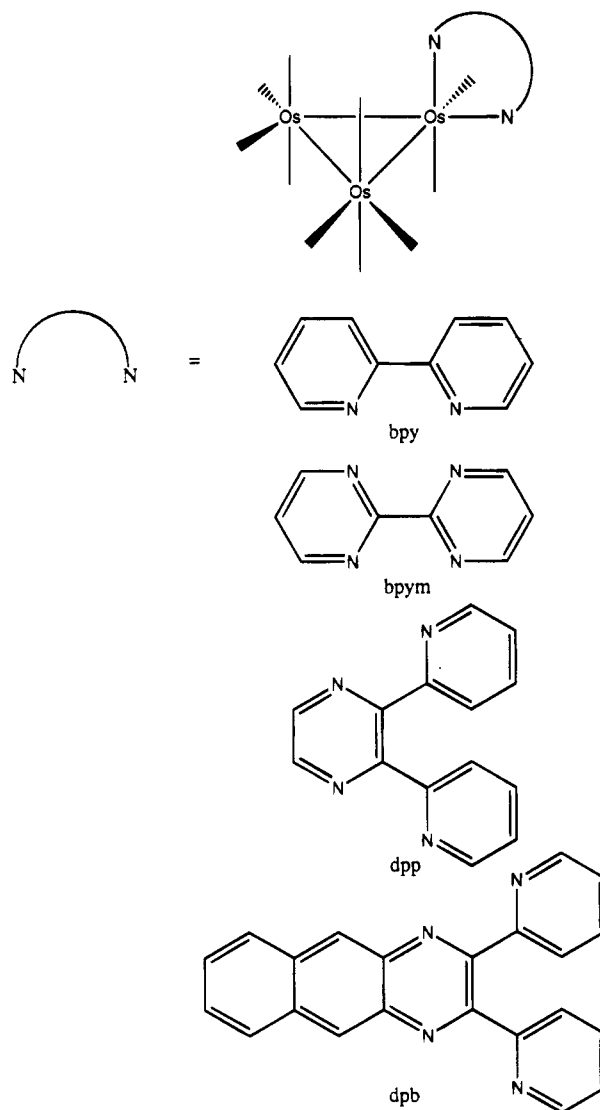


Figure 1. Schematic structure of the complexes $\text{Os}_3(\text{CO})_{10}(\text{L})$ and of the ligands L used.

excitation of the sample by a Spectra Physics Model 2025 argon ion or Spectra Physics DCR-11 Nd:YAG laser. Low-temperature IR and UV-vis measurements were performed using an Oxford Instruments DN 1704/54 liquid nitrogen cryostat with CaF_2 and quartz windows. $^1\text{H-NMR}$ spectra were recorded on a Bruker AMX 300 spectrometer and ESR spectra on a Varian E6 spectrometer with a 100 kHz modulation. Raman measurements were performed using a Dilor Modular XY system with a multichannel diode array detection system. Spectra were obtained by excitation with a Spectra Physics Model 2016 argon ion laser and a Coherent CR 490 dye laser using Coumarin or Rhodamin 6G as a dye.

Nanosecond time-resolved absorption spectra were obtained using a Spectra Physics GCR-3 Nd:YAG laser as the excitation source. The 1064 nm fundamental yielded 5 ns pulses at a maximum of 10 pulses/s. The required 532 nm pulse was obtained by frequency doubling using KDP crystals. A right-angle optical system was used for the excitation-analyzing setup. A 450 W high-pressure xenon lamp was used as the probe light. In order to enhance its brightness during the observation time gate of the detector, the xenon lamp was pulsed with a Müller Elektronik MSP 05 pulser. The probe light, after passing through the sample cell, was dispersed via a spectrograph (EG & G Model 1234) equipped with a 150 g/mm grating and a 250 μm slit, resulting in a 6 nm spectral resolution. The data collection system consisted of an EG & G Model 1460 OMA-III console provided with a 1302 fast pulser (gate width, 5 ns) and an EG & G Model 1421 gated diode array detector.

Picosecond laser flash photolysis measurements were performed using the equipment^{32,33} of the Canadian Centre for Picosecond Laser

- (24) Kaupp, K.; Stoll, H.; Preuss, H.; Kaim, W.; Stahl, T.; van Koten, G.; Wissing, E.; Smeets, W. J.; Spek, A. L. *J. Am. Chem. Soc.* **1991**, *113*, 5606.
- (25) Rossenaar, B. D.; Kleverlaan, C. J.; Stufkens, D. J.; Oskam, A. *J. Chem. Soc., Chem. Commun.* **1994**, 63.
- (26) Nieuwenhuis, H. A.; van de Ven, M. C. E.; Stufkens, D. J.; Oskam, A.; Goubitz, K. *Organometallics* **1995**, *14*, 780.
- (27) Djurovich, P. I.; Watts, R. J. *Inorg. Chem.* **1993**, *32*, 4681.
- (28) Djurovich, P. I.; Watts, R. J. *J. Phys. Chem.* **1994**, *98*, 396.
- (29) Djurovich, P. I.; Cook, W.; Joshi, R.; Watts, R. J. *J. Phys. Chem.* **1994**, *98*, 398.
- (30) Zoet, R.; Jastrzebski, J. T. B. H.; van Koten, G.; Mahabiersing, T.; Vrieze, K.; Heijdenrijk, D.; Stam, C. H. *Organometallics* **1988**, *7*, 2108.
- (31) Baiano, J. A.; Carlson, D. L.; Wolosh, G. M.; DeJesus, D. E.; Knowles, C. F.; Szabo, E. G.; Murphy, W. R. *Inorg. Chem.* **1990**, *29*, 2327.

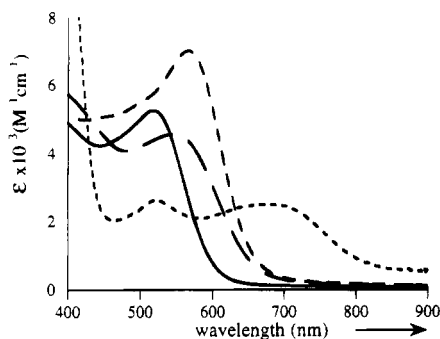


Figure 2. UV-vis spectra of $\text{Os}_3(\text{CO})_{10}(\text{L})$ ($\text{L} = \text{bpy}$ (—), bpym (---), dpp (- · -), dpb (····)) in THF at 293 K.

Table 1. Absorption Maxima of $\text{Os}_3(\text{CO})_{10}(\text{L})$ in Different Solvents

compound	λ (nm)		
	toluene	THF (ϵ ($\text{M}^{-1} \text{cm}^{-1}$))	acetonitrile
$\text{Os}_3(\text{CO})_{10}(\text{bpy})$	490, 557	493, 527 (5260)	516
$\text{Os}_3(\text{CO})_{10}(\text{bpym})$	388, 586	393, 551 (4560)	392, 547
$\text{Os}_3(\text{CO})_{10}(\text{dpp})$	527, 595	514, 571 (7030)	514, 565
$\text{Os}_3(\text{CO})_{10}(\text{dpb})$	490 (sh), 532, 667 (sh), 722	522, 694 (2500)	389 (sh), 518, 669 (br)

Spectroscopy at Concordia University, Montreal. The sample was excited at 532 nm with 30 ps (fwhm), ≈ 2 mJ pulses of a Q-switched Quantel YG 402 G Nd:YAG laser. Transient absorption spectra were measured at selected delay times after the sample excitation using probe pulses of a white continuum (425–675 nm) generated by focusing part of the fundamental laser beam on a cell with D_3PO_4 . Delay times between the excitation and probe pulses were varied in the 0 ps to 10 ns range. The data were collected using an EG&G PAR OMA II console with a silicon-enhanced vidicon array detector. Difference transient absorption spectra were obtained by subtracting the spectra measured with and without previous sample excitation. Each spectrum is an average of 8–10 measurements. The sample solutions were placed in a 2 mm quartz cell and well-stirred between laser excitations. Sample absorbance at the excitation wavelength was maintained in the range 0.3–0.6.

Continuous wave photochemistry was carried out by irradiating solutions of the complexes with a Spectra Physics Model 2025 argon ion laser.

Elemental analyses were performed by the Mikroanalytisches Laboratorium of Dornis und Kolbe, Mülheim a.d. Ruhr, Germany.

Results

Spectroscopic Properties. (a) UV-vis Spectroscopy. The absorption spectra of $\text{Os}_3(\text{CO})_{10}(\text{L})$ in the wavelength region 300–900 nm are presented in Figure 2, and the absorption maxima are collected in Table 1.

The osmium clusters all show an unstructured absorption band in the visible region, whose position depends on the α -diimine ligand. It shifts to lower energy when the energy of the lowest π^* orbital of the α -diimine decreases in the order $\text{bpy} > \text{bpym} > \text{dpp} > \text{dpb}$. This effect agrees with the MLCT character of the electronic transitions, which is also evident from their solvatochromism (see Table 1).

(b) Resonance Raman Spectroscopy. Resonance Raman (RR) spectroscopy is a very valuable technique for the assignment of allowed electronic transitions.^{34,35} Since only those

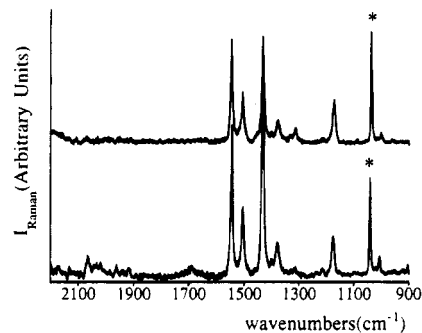


Figure 3. Resonance Raman spectra of $\text{Os}_3(\text{CO})_{10}(\text{bpym})$ in KNO_3 (*) at room temperature. Excitation wavelength: 514.5 nm (top), 550 nm (bottom).

Table 2. Resonance Enhanced Raman Bands of $\text{Os}_3(\text{CO})_{10}(\text{L})$ in the Region 900–2100 cm^{-1} , Measured in KNO_3 at 293 K, $\lambda_{\text{exc}} = 514.5$ nm

compound	Raman bands (cm^{-1})
$\text{Os}_3(\text{CO})_{10}(\text{bpy})$	2081, 1602, 1555, 1485, 1322, 1173
$\text{Os}_3(\text{CO})_{10}(\text{bpym})$	2087, 1578, 1537, 1463, 1194
$\text{Os}_3(\text{CO})_{10}(\text{dpp})$	2088, 1550, 1514, 1470
$\text{Os}_3(\text{CO})_{10}(\text{dpb})$	2088, 1513, 1462, 1361

vibrations will resonantly be enhanced, which are vibronically coupled to the electronic transitions, these transitions can be characterized by the observed RR effects. RR spectra of the complexes were recorded in a KNO_3 disk, with exciting laser lines ranging from 457.9 to 620 nm. The main resonantly enhanced Raman bands in the region 1000–2100 cm^{-1} are collected in Table 2. Figure 3 presents the Raman spectra of $\text{Os}_3(\text{CO})_{10}(\text{bpym})$ obtained by excitation at two different excitation wavelengths into the first absorption band.

The Raman bands can be assigned by comparison with literature data on closely related complexes.^{36–38} The spectra of all complexes show resonance enhancement of Raman intensity for several bands in the 1400–1600 cm^{-1} region which belong to a combination of C=C and C=N stretchings. In addition, a weak RR effect is observed for a $\nu_s(\text{CO})$ vibration at ca. 2090 cm^{-1} .

Photochemistry. When the complexes were irradiated into their lowest-energy absorption band at room temperature, and in the absence of a reactant, no photoproduct was obtained and no photoreaction was observed with conventional spectroscopic (UV-vis, IR) techniques. In order to find out if the photostability was caused by the inertness of the excited state or by a fast and complete back-reaction of an intermediate to the parent complex, photoreactions were followed at room temperature with rapid scan FTIR and pico- and nanosecond time-resolved UV-vis spectroscopy and also performed at low temperatures.

(a) Rapid Scan FTIR Spectroscopy. Rapid scan FTIR spectroscopy is a valuable technique to follow reactions on a millisecond to second time scale. Spectral changes are studied either with continuous irradiation or after excitation with a short light pulse. In the present study, photoreactions in different solvents were followed during continuous irradiation by an argon ion laser. The IR spectral results strongly depended on the coordinating properties of the solvent. Thus, in toluene and THF, no photoreaction was observed, just as in the case of the conventional IR experiments. However, a photoreaction occurred upon irradiation of the complexes in CH_3CN . The IR

(32) Langford, C. H.; Moralejo, C.; Sharma, D. K. *Inorg. Chim. Acta* **1987**, 126, 111.

(33) Lindsay, E.; Vlček, A., Jr.; Langford, C. H. *Inorg. Chem.* **1993**, 32, 3822.

(34) Balk, R. W.; Stufkens, D. J.; Oskam, A. *J. Chem. Soc., Dalton Trans.* **1981**, 1124.

(35) Balk, R. W.; Snoeck, T. L.; Stufkens, D. J.; Oskam, A. *Inorg. Chem.* **1980**, 19, 3015.

(36) McClanahan, S.; Kincaid, J. J. *J. Raman Spectrosc.* **1984**, 15, 173.

(37) Braunstein, C. H.; Baker, A. D.; Strekas, T. C.; Gafney, H. D. *Inorg. Chem.* **1984**, 23, 857.

(38) Kaim, W.; Kohlmann, S.; Lees, A.; Snoeck, T. L.; Stufkens, D. J.; Zulu, M. M. *Inorg. Chim. Acta* **1993**, 210, 159.

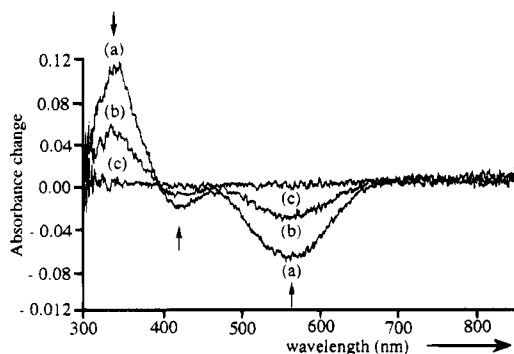


Figure 4. Difference absorption spectra measured 20 (a), 270 (b), and 970 ns (c) after 532 nm, 5 ns excitation of a solution of Os₃(CO)₁₀(bpy) in THF at 293 K.

Table 3. Lifetimes (ns) of the Transient Species in Various Media

parent complex	lifetime		
	toluene	THF	CH ₃ CN
Os ₃ (CO) ₁₀ (bpy) ^a	<10	246	6.5 × 10 ⁹
Os ₃ (CO) ₁₀ (bpym)	<10	568	(15–20) × 10 ⁹
Os ₃ (CO) ₁₀ (dpp)	<10	914	16 × 10 ⁹

^a $\tau = 12 \times 10^{11}$ ns in pyridine.

bands of the starting complex decreased in intensity, and new bands of a single photoproduct showed up. When about half of the starting material was converted, a photostationary state was reached, and when the irradiation was stopped, the photoproduct started to react back to give the parent compound. From this back-reaction, the lifetime of the photoproduct was calculated from the decrease of its 1875 cm⁻¹ band according to first order kinetics. Table 3 presents the lifetimes of all photoproducts, their IR frequencies are collected in Table 4.

It is clear from these rapid scan results that the photoreactions in less coordinating solvents can only be studied on a shorter time scale. For this purpose the experiments were extended to nanosecond and picosecond transient absorption spectroscopy.

(b) Nanosecond Transient UV-vis Absorption Spectroscopy. Transient absorption spectra were measured after excitation of the complexes by 5 ns pulses of the 532 nm line of a Nd:YAG laser. For all complexes, the lifetime of the transient species was less than 10 ns in toluene but much longer when measured in THF. This is demonstrated by the data in Table 3 and by the difference absorption spectra of Os₃(CO)₁₀(bpy) in THF, measured 20, 270, and 970 ns after excitation with $\lambda = 532$ nm (Figure 4). Both the bleaching at 560 and 420 nm and the transient absorption at 350 nm disappeared with the same lifetime of 568 ns. The lifetimes were calculated from the intensity decrease of the transient absorption spectrum at three different wavelengths according to first order kinetics. The lifetimes collected in Table 3 do not only depend on the coordinating ability of the solvent but also on the α -diimine. It is especially the energy of the lowest π^* orbital, which decreases in the order bpy > bpym > dpp according to the reduction potentials,³⁹ that influences this lifetime.

The absorption maxima of the transient species in THF are collected in Table 5. They were obtained by correcting the difference absorption spectra for the spectra of the parent complexes. These maxima are somewhat shifted to shorter wavelengths with respect to the parent compounds.

The complex Os₃(CO)₁₀(dpp) also showed the formation of a transient species, but its band pattern differed from that of the transient species observed for the other complexes. More-

(39) van Outersterp, J. W. M.; Garriga Oostenbrink, M. T.; Hartl, F.; Stufkens, D. J. To be published.

Table 4. CO-Stretching Frequencies of Os₃(CO)₁₀(L) and Their Photoproducts in Various Media

compound	medium (T (K))	$\nu(\text{CO})$ (cm ⁻¹)
Os ₃ (CO) ₁₀ (bpy) Os ₃ (CO) ₁₀ (bpy) photoproduct (bpy)	THF (293)	1953 m
	2-MeTHF (133)	1958 sh
	2-MeTHF (133)	1947 w
	CH ₃ CN (293)	1901 m
Os ₃ (CO) ₁₀ (bpym) Os ₃ (CO) ₁₀ (bpym) photoproduct(bpym)	THF/NBu ₄ Br (293)	1951 m
	2-MeTHF (133)	1922 w
	2-MeTHF (133)	1915 w
	CH ₃ CN (293)	1890 w
Os ₃ (CO) ₁₀ (dpp) Os ₃ (CO) ₁₀ (dpp) photoproduct(dpp)	THF/NBu ₄ Br (293)	1907 m
	2-MeTHF (133)	1903 m
	2-MeTHF (133)	1899 w
	CH ₃ CN (293)	1898 w
Os ₃ (CO) ₁₀ (dpp) Os ₃ (CO) ₁₀ (dpp) photoproduct(dpp)	THF/NBu ₄ Br (293)	1924 w
	2-MeTHF (133)	1925 w
	2-MeTHF (133)	1921 w
	CH ₃ CN (293)	1900 w
Os ₃ (CO) ₁₀ (dpp) Os ₃ (CO) ₁₀ (dpp) photoproduct(dpp)	THF/NBu ₄ Br (293)	1957 m
	2-MeTHF (133)	1951 m
	2-MeTHF (133)	1956 sh
	CH ₃ CN (293)	1953 sh
Os ₃ (CO) ₁₀ (dpp) Os ₃ (CO) ₁₀ (dpp) photoproduct(dpp)	THF/NBu ₄ Br (293)	1968 m
	2-MeTHF (133)	1968 m
	2-MeTHF (133)	1965 s, br
	CH ₃ CN (293)	1969 sh
Os ₃ (CO) ₁₀ (dpp) Os ₃ (CO) ₁₀ (dpp) photoproduct(dpp)	THF/NBu ₄ Br (293)	1979 s
	2-MeTHF (133)	1979 s
	2-MeTHF (133)	1977 s
	CH ₃ CN (293)	1977 s
Os ₃ (CO) ₁₀ (dpp) Os ₃ (CO) ₁₀ (dpp) photoproduct(dpp)	THF/NBu ₄ Br (293)	1986 m
	2-MeTHF (133)	1986 m
	2-MeTHF (133)	1988 m
	CH ₃ CN (293)	1988 m
Os ₃ (CO) ₁₀ (dpp) Os ₃ (CO) ₁₀ (dpp) photoproduct(dpp)	THF/NBu ₄ Br (293)	1996 m
	2-MeTHF (133)	1996 m
	2-MeTHF (133)	1996 m
	CH ₃ CN (293)	1996 m
Os ₃ (CO) ₁₀ (dpp) Os ₃ (CO) ₁₀ (dpp) photoproduct(dpp)	THF/NBu ₄ Br (293)	2011 s
	2-MeTHF (133)	2011 s
	2-MeTHF (133)	2011 s
	CH ₃ CN (293)	2011 s
Os ₃ (CO) ₁₀ (dpp) Os ₃ (CO) ₁₀ (dpp) photoproduct(dpp)	THF/NBu ₄ Br (293)	2032 s
	2-MeTHF (133)	2032 s
	2-MeTHF (133)	2034 s
	CH ₃ CN (293)	2034 s
Os ₃ (CO) ₁₀ (dpp) Os ₃ (CO) ₁₀ (dpp) photoproduct(dpp)	THF/NBu ₄ Br (293)	2064 w
	2-MeTHF (133)	2065 w
	2-MeTHF (133)	2068 w
	CH ₃ CN (293)	2068 w
Os ₃ (CO) ₁₀ (dpp) Os ₃ (CO) ₁₀ (dpp) photoproduct(dpp)	THF/NBu ₄ Br (293)	2066 m
	2-MeTHF (133)	2067 s
	2-MeTHF (133)	2069 w
	CH ₃ CN (293)	2069 w
Os ₃ (CO) ₁₀ (dpp) Os ₃ (CO) ₁₀ (dpp) photoproduct(dpp)	THF/NBu ₄ Br (293)	2077 w
	2-MeTHF (133)	2077 w
	2-MeTHF (133)	2077 w
	CH ₃ CN (293)	2077 w
Os ₃ (CO) ₁₀ (dpp) Os ₃ (CO) ₁₀ (dpp) photoproduct(dpp)	THF/NBu ₄ Br (293)	2083 w
	2-MeTHF (133)	2083 w
	2-MeTHF (133)	2083 w
	CH ₃ CN (293)	2083 w
Os ₃ (CO) ₁₀ (dpp) Os ₃ (CO) ₁₀ (dpp) photoproduct(dpp)	THF/NBu ₄ Br (293)	2088 w
	2-MeTHF (133)	2088 w
	2-MeTHF (133)	2088 w
	CH ₃ CN (293)	2088 w
Os ₃ (CO) ₁₀ (dpp) Os ₃ (CO) ₁₀ (dpp) photoproduct(dpp)	THF/NBu ₄ Br (293)	2090 m
	2-MeTHF (133)	2090 m
	2-MeTHF (133)	2090 m
	CH ₃ CN (293)	2090 m
Os ₃ (CO) ₁₀ (dpp) Os ₃ (CO) ₁₀ (dpp) photoproduct(dpp)	THF/NBu ₄ Br (293)	2099 sh
	2-MeTHF (133)	2099 sh
	2-MeTHF (133)	2099 sh
	CH ₃ CN (293)	2099 sh
Os ₃ (CO) ₁₀ (dpp) Os ₃ (CO) ₁₀ (dpp) photoproduct(dpp)	THF/NBu ₄ Br (293)	2101 m
	2-MeTHF (133)	2101 m
	2-MeTHF (133)	2101 m
	CH ₃ CN (293)	2101 m
Os ₃ (CO) ₁₀ (dpp) Os ₃ (CO) ₁₀ (dpp) photoproduct(dpp)	THF/NBu ₄ Br (293)	2115 m
	2-MeTHF (133)	2115 m
	2-MeTHF (133)	2115 m
	CH ₃ CN (293)	2115 m
Os ₃ (CO) ₁₀ (dpp) Os ₃ (CO) ₁₀ (dpp) photoproduct(dpp)	THF/NBu ₄ Br (293)	2044 m
	2-MeTHF (133)	2044 m
	2-MeTHF (133)	2044 m
	CH ₃ CN (293)	2044 m
Os ₃ (CO) ₁₀ (dpp) Os ₃ (CO) ₁₀ (dpp) photoproduct(dpp)	THF/NBu ₄ Br (293)	2036 m
	2-MeTHF (133)	2036 m
	2-MeTHF (133)	2036 m
	CH ₃ CN (293)	2036 m
Os ₃ (CO) ₁₀ (dpp) Os ₃ (CO) ₁₀ (dpp) photoproduct(dpp)	THF/NBu ₄ Br (293)	2084 m
	2-MeTHF (133)	2084 m
	2-MeTHF (133)	2085 m
	CH ₃ CN (293)	2085 m
Os ₃ (CO) ₁₀ (dpp) Os ₃ (CO) ₁₀ (dpp) photoproduct(dpp)	THF/NBu ₄ Br (293)	2087 w
	2-MeTHF (133)	2087 w
	2-MeTHF (133)	2087 w
	CH ₃ CN (293)	2087 w
Os ₃ (CO) ₁₀ (dpp) Os ₃ (CO) ₁₀ (dpp) photoproduct(dpp)	THF/NBu ₄ Br (293)	2073 w
	2-MeTHF (133)	2073 w
	2-MeTHF (133)	2073 w
	CH ₃ CN (293)	2073 w
Os ₃ (CO) ₁₀ (dpp) Os ₃ (CO) ₁₀ (dpp) photoproduct(dpp)	THF/NBu ₄ Br (293)	2086 m
	2-MeTHF (133)	2086 m
	2-MeTHF (133)	2086 m
	CH ₃ CN (293)	2086 m
Os ₃ (CO) ₁₀ (dpp) Os ₃ (CO) ₁₀ (dpp) photoproduct(dpp)	THF/NBu ₄ Br (293)	2079 w
	2-MeTHF (133)	2079 w
	2-MeTHF (133)	2079 w
	CH ₃ CN (293)	2079 w
Os ₃ (CO) ₁₀ (dpp) Os ₃ (CO) ₁₀ (dpp) photoproduct(dpp)	THF/NBu ₄ Br (293)	2083 w
	2-MeTHF (133)	2083 w
	2-MeTHF (133)	2083 w
	CH ₃ CN (293)	2083 w
Os ₃ (CO) ₁₀ (dpp) Os ₃ (CO) ₁₀ (dpp) photoproduct(dpp)	THF/NBu ₄ Br (293)	2088 w
	2-MeTHF (133)	2088 w
	2-MeTHF (133)	2088 w
	CH ₃ CN (293)	2088 w
Os ₃ (CO) ₁₀ (dpp) Os ₃ (CO) ₁₀ (dpp) photoproduct(dpp)	THF/NBu ₄ Br (293)	2083 vw
	2-MeTHF (133)	2083 vw
	2-MeTHF (133)	2083 vw
	CH ₃ CN (293)	2083 vw
Os ₃ (CO) ₁₀ (dpp) Os ₃ (CO) ₁₀ (dpp) photoproduct(dpp)	THF/NBu ₄ Br (293)	2074 w
	2-MeTHF (133)	2074 w
	2-MeTHF (133)	2074 w
	CH ₃ CN (293)	2074 w
Os ₃ (CO) ₁₀ (dpp) Os ₃ (CO) ₁₀ (dpp) photoproduct(dpp)	THF/NBu ₄ Br (293)	2083 w
	2-MeTHF (133)	2083 w
	2-MeTHF (133)	2083 w
	CH ₃ CN (293)	2083 w
Os ₃ (CO) ₁₀ (dpp) Os ₃ (CO) ₁₀ (dpp) photoproduct(dpp)	THF/NBu ₄ Br (293)	2088 m
	2-MeTHF (133)	2088 m
	2-MeTHF (133)	2088 m
	CH ₃ CN (293)	2088 m
Os ₃ (CO) ₁₀ (dpp) Os ₃ (CO) ₁₀ (dpp) photoproduct(dpp)	THF/NBu ₄ Br (293)	2083 w
	2-MeTHF (133)	2083 w
	2-MeTHF (133)	2083 w
	CH ₃ CN (293)	2083 w
Os ₃ (CO) ₁₀ (dpp) Os ₃ (CO) ₁₀ (dpp) photoproduct(dpp)	THF/NBu ₄ Br (293)	2083 w
	2-MeTHF (133)	2083 w
	2-MeTHF (133)	2083 w
	CH ₃ CN (293)	2083 w
Os ₃ (CO) ₁₀ (dpp) Os ₃ (CO) ₁₀ (dpp) photoproduct(dpp)	THF/NBu ₄ Br (293)	2083 w
	2-MeTHF (133)	2083 w
	2-MeTHF (133)	2083 w
	CH ₃ CN (293)	2083 w
Os ₃ (CO) ₁₀ (dpp) Os ₃ (CO) ₁₀ (dpp) photoproduct(dpp)	THF/NBu ₄ Br (293)	2083 w
	2-MeTHF (133)	2083 w
	2-MeTHF (133)	2083 w
	CH ₃ CN (293)	2083 w
Os ₃ (CO) ₁₀ (dpp) Os ₃ (CO) ₁₀ (dpp) photoproduct(dpp)	THF/NBu ₄ Br (293)	2083 w
	2-MeTHF (133)	2083 w
	2-MeTHF (133)	2083 w
	CH ₃ CN (293)	2083 w
Os ₃ (CO) ₁₀ (dpp) Os ₃ (CO) ₁₀ (dpp) photoproduct(dpp)	THF/NBu ₄ Br (293)	2083 w
	2-MeTHF (133)	2083 w
	2-MeTHF (133)	2083 w
	CH ₃ CN (293)	2083 w
Os ₃ (CO) ₁₀ (dpp) Os ₃ (CO) ₁₀ (dpp) photoproduct(dpp)	THF/NBu ₄ Br (293)	2083 w
	2-MeTHF (133)	2083 w
	2-MeTHF (133)	2083 w
	CH ₃ CN (293)	2083 w
Os ₃ (CO) ₁₀ (dpp) Os ₃ (CO) ₁₀ (dpp) photoproduct(dpp)	THF/NBu ₄ Br (293)	2083 w
	2-MeTHF (133)	2083 w
	2-MeTHF (133)	2083 w
	CH ₃ CN (293)	2083 w
Os ₃ (CO) ₁₀ (dpp) Os ₃ (CO) ₁₀ (dpp) photoproduct(dpp)	THF/NBu ₄ Br (293)	2083 w
	2-MeTHF (133)	2083 w
	2-MeTHF (133)	2083 w
	CH ₃ CN (293)	2083 w
Os ₃ (CO) ₁₀ (dpp) Os ₃ (CO) ₁₀ (dpp) photoproduct(dpp)	THF/NBu ₄ Br (293)	2083 w
	2-MeTHF (133)	2083 w
	2-MeTHF (133)	2083 w
	CH ₃ CN (293)	2083 w
Os ₃ (CO) ₁₀ (dpp) Os ₃ (CO) ₁₀ (dpp) photoproduct(dpp)	THF/NBu ₄ Br (293)	2083 w
	2-MeTHF (133)	2083 w
	2-MeTHF (133)	2083 w
	CH ₃ CN (293)	2083 w
Os ₃ (CO) ₁₀ (dpp) Os ₃ (CO) ₁₀ (dpp) photoproduct(dpp)	THF/NBu ₄ Br (293)	2083 w
	2-MeTHF (133)	2083 w
	2-MeTHF (133)	2083 w
	CH ₃ CN (293)	2083 w
Os ₃ (CO) ₁₀ (dpp) Os ₃ (CO) ₁₀ (dpp) photoproduct(dpp)	THF/NBu ₄ Br (293)	2083 w
	2-MeTHF (133)	2083 w
	2-MeTHF (133)	2083 w
	CH ₃ CN (293)	2083 w
Os ₃ (CO) ₁₀ (dpp) Os ₃ (CO) ₁₀ (dpp) photoproduct(dpp)	THF/NBu ₄ Br (293)	2083 w
	2-MeTHF (133)	2083 w
	2-MeTHF (133)	2083 w
	CH ₃ CN (293)	2083 w
Os ₃ (CO) ₁₀ (dpp) Os ₃ (CO) ₁₀ (dpp) photoproduct(dpp)	THF/NBu ₄ Br (293)	2083 w
	2-MeTHF (133)	2083 w
	2-MeTHF (133)	2083 w
	CH ₃ CN (293)	2083 w
Os ₃ (CO) ₁₀ (dpp) Os ₃ (CO) ₁₀ (dpp) photoproduct(dpp)	THF/NBu ₄ Br (293)	2083 w
	2-MeTHF (133)	2083 w
	2-MeTHF (133)	2083 w
	CH ₃ CN (293)	2083 w
Os ₃ (CO) ₁₀ (dpp) Os ₃ (CO) ₁₀ (dpp) photoproduct(dpp)	THF/NBu ₄ Br (293)	2083 w
	2-MeTHF (133)	2083 w
	2-MeTHF (133)	2083 w
	CH ₃ CN (293)	2083 w
Os ₃ (CO) ₁₀ (dpp) Os ₃ (CO) ₁₀ (dpp) photoproduct(dpp)	THF/NBu ₄ Br (293)	2083 w
	2-MeTHF (133)	2083 w
	2-MeTHF (133)	2083 w
	CH ₃ CN (293)	2083 w
Os ₃ (CO) ₁₀ (dpp) Os ₃ (CO) ₁₀ (dpp) photoproduct(dpp)	THF/NBu ₄ Br (293)	2083 w
	2-MeTHF (133)	2083 w
	2-MeTHF (133)	2083 w
	CH ₃ CN (293)	2083 w
Os ₃ (CO) ₁₀ (dpp) Os ₃ (CO) ₁₀ (dpp) photoproduct(dpp)	THF/NBu ₄ Br (293)	

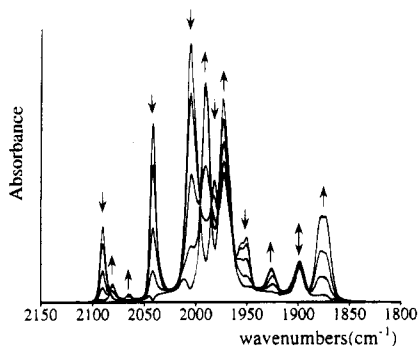


Figure 5. IR spectral changes upon photolysis of $\text{Os}_3(\text{CO})_{10}(\text{dpp})$ in 2-MeTHF (133 K): $\lambda_{\text{exc}} = 514.5$ nm.

Table 5. UV-vis Data of the Photoproducts of $\text{Os}_3(\text{CO})_{10}(\text{L})$ in Various Media

parent complex	THF (293 K)	2-MeTHF (133 K)	THF/ Bu_4NBr (293 K)	aceto- nitrile (293 K)	THF/ $\text{P}(\text{OMe})_3$ (173 K)
$\text{Os}_3(\text{CO})_{10}(\text{bpy})$	423	564 (183 K)		601	563
$\text{Os}_3(\text{CO})_{10}(\text{bpym})$	447	612	576	631	
$\text{Os}_3(\text{CO})_{10}(\text{dpp})$	470	600	629	660	612

over, its lifetime was much shorter (~ 10 ns in THF) than expected on the basis of the energy of its lowest π^* orbital.

(c) Picosecond Time-Resolved UV-vis Absorption Spectroscopy. Picosecond transient absorption spectra were measured for $\text{Os}_3(\text{CO})_{10}(\text{bpy})$ dissolved in THF in the wavelength region 425–675 nm. No such spectra could be obtained in toluene due to the low solubility of the complex in this solvent. The spectra were measured at several probe delays between 0 ps and 10 ns after excitation by 30 ps pulses of the 532 nm line of the Nd:YAG laser. The same difference absorption spectra were obtained at probe delays of 50 ps and 10 ns, and these spectra also did not deviate from those obtained for this complex in the nanosecond time-resolved measurements. The spectra show bleaching at ca. 500 nm, which corresponds to depletion of the ground state. There is no evidence for a prominent transient absorption between 500 and 675 nm but a small increase of absorption below 475 nm.

(d) Low-Temperature Photoreactions. Upon photolysis in 2-MeTHF at 133 K, the complexes $\text{Os}_3(\text{CO})_{10}(\text{L})$ ($\text{L} = \text{bpy}$, bpym , dpp) transformed into stable photoproducts, the IR and UV-vis data of which are collected in Tables 4 and 5, respectively. The IR spectral changes, accompanying this photoreaction in the case of $\text{Os}_3(\text{CO})_{10}(\text{dpp})$, are shown in Figure 5. The IR pattern of the photoproduct is completely different from that of the starting material, which means that both compounds have a different structure. For the complex $\text{Os}_3(\text{CO})_{10}(\text{dpp})$, no reaction was observed, not even at this low temperature.

When the temperature was raised to 293 K after completion of the photoreaction, the starting material was almost completely recovered. This back-reaction was also evident from the photostationary state that was reached upon photolysis above 133 K. The temperature has a large influence not only on the lifetime of the photoproduct but also on the position of its first absorption band (Figure 6). Going from room temperature in THF to 133 K in 2-MeTHF, this band shifts appreciably to lower energy. This effect, which points to the presence of a coordinatively unsaturated chromophore, will be discussed hereafter.

In dichloromethane, a polar but noncoordinating solvent, a photoreaction occurred at 193 K, but the photoproduct was different from that formed in 2-MeTHF. Moreover, it did not react back to give the starting compound upon raising the

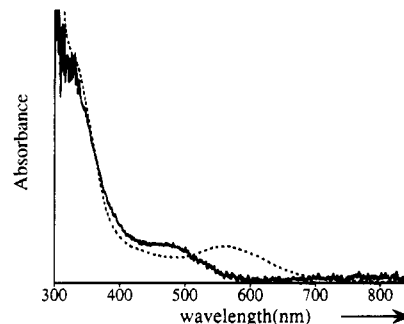


Figure 6. UV-vis spectra of the photoproducts of $\text{Os}_3(\text{CO})_{10}(\text{dpp})$ at 293 K in THF (—) (obtained by adding the UV-vis spectrum of $\text{Os}_3(\text{CO})_{10}(\text{dpp})$ to the difference absorption spectrum measured 20 ns after 532 nm, 5 ns excitation) and at 133 K in 2-MeTHF (.....).

temperature to 293 K. Performing the reaction in toluene at 193 K did not give rise to the formation of any photoproduct.

(e) Photoreactions with $\text{P}(\text{OMe})_3$, Bu_4NX , and AlCl_3 . The above experiments demonstrate that the lifetimes of the photoproducts are strongly dependent on the coordinating properties of the solvent. In order to get more insight into this stabilizing effect, the photoreactions of the clusters were also studied in the presence of a variety of reactants, including radical scavengers. In the presence of a radical scavenger, such as *t*-BuNO (2-methyl-2-nitrosopropane dimer) or CCl_4 , or a reactant, such as $\text{P}(\text{OMe})_3$, no photoreaction was observed by conventional spectroscopic techniques. In the case of CCl_4 and $\text{P}(\text{OMe})_3$ a thermal reaction occurred instead. Attempts to observe an ESR signal in both the absence and presence of a radical scavenger failed, even when the temperature was lowered to 173 K. In order to avoid the above mentioned thermal reaction, the photoreaction with $\text{P}(\text{OMe})_3$ was performed at 173 K in 2-MeTHF in a dedicated free access IR (FAIR) cell⁴⁰ in which a solution of the complex was first cooled before a 100-fold excess of $\text{P}(\text{OMe})_3$ was added. Upon irradiation, a stable product was formed that showed a similar IR pattern as the products formed without $\text{P}(\text{OMe})_3$ in THF/2-MeTHF (low-temperature) and CH_3CN (rapid scan) (Table 4). In contrast to these latter products, the reaction products of $\text{P}(\text{OMe})_3$ were thermally stable and did not react back to the parent complexes upon raising the temperature to 293 K. When the photoreaction was performed in the presence of an ammonium salt such as $\text{Bu}_4\text{N}^+\text{X}^-$ ($\text{X}^- = \text{halide}$), a product was formed ($\phi \cong 5 \times 10^{-2}$) which had the same IR pattern in the CO-stretching region as the photoproduct obtained by irradiation at low temperatures in 2-MeTHF or THF. It is noteworthy that also this photoproduct is completely stable at room temperature.

Upon irradiation of $\text{Os}_3(\text{CO})_{10}(\text{dpp})$ in the presence of the Lewis acid AlCl_3 , the IR pattern of the cluster was preserved, but the CO-vibrations were shifted to higher frequencies (Table 4). This means that the electron density at the cluster was diminished.

(f) Spectroscopic Properties of the Photoproducts. It is clear that the photoproducts obtained as transient species in THF or acetonitrile, as stable complexes in THF or 2-MeTHF at low temperature, or in the presence of $\text{P}(\text{OMe})_3$ or Bu_4NX at room temperature, are of similar structure. In order to resolve this structure, we studied the RR spectra of the photoproduct of $\text{Os}_3(\text{CO})_{10}(\text{bpym})$ at low temperatures in THF. For this purpose the photoconversion of this cluster into the photoproduct was first followed with IR. When maximal conversion was reached, the RR spectrum of the photoproduct was measured by

(40) Schilder, P. G. M.; Luyten, H.; Stufkens, D. J.; Oskam, A. *Appl. Spectrosc.* 1991, 45, 1344.

excitation with 514.5 nm. In the frequency region 1400–1650 cm^{-1} , the bpm-stretching modes occurred at higher frequencies than those for the parent complex. For $\text{Os}_3(\text{CO})_{10}(\text{bpy})$, they were observed at 1577, 1536, and 1464 cm^{-1} , whereas for the photoproduct at 1605, 1560, and 1491 cm^{-1} . The occurrence of such a high-frequency shift of the bpm-vibrations with retention of the Raman intensity pattern indicates that the photoproduct still contains an Os–bpy moiety, in which the Os atom has, however, a higher positive charge. The presence of the radical anion $\text{bpy}^{\cdot-}$ in the photoproduct could be excluded here. In that case the bpm-vibrations would have shifted to lower frequency with respect to the parent complex, just as for $\text{W}(\text{CO})_4(\text{bpy})$. For this latter complex, the ligand vibrations shifted from 1577 and 1548 cm^{-1} to 1570 and 1511 cm^{-1} upon reduction.³⁸

In order to get more information about the structure of the photoproduct, the photoreaction of $\text{Os}_3(\text{CO})_{10}(\text{bpy})$ in deuterated pyridine with continuous 500 nm irradiation was followed by $^1\text{H-NMR}$ spectroscopy. From the spectra it was evident that the bands of the photoproduct were shifted approximately 0.20 ppm downfield. Such a downfield shift supports our tentative conclusion from the RR spectra that the photoproducts of the osmium clusters have a more positively charged osmium atom adjacent to the neutral α -diimine ligand.

Discussion

The assignment of the lowest-energy absorption band of these complexes (Figure 2) is straightforward. Its maximum depends on the α -diimine ligand in such a way that it shifts to lower energy when the energy of its lowest π^* orbital decreases in the order $\text{bpy} > \text{bpy} > \text{dpp} > \text{dpb}$. Because of this strong influence of the π^* orbital energy on the absorption maximum, these bands most likely belong to $\text{Os} \rightarrow \alpha$ -diimine (MLCT) transitions. This assignment agrees with the high extinction coefficients and the solvatochromism of these bands. It is confirmed by the RR spectra, which show resonance enhancement of the intensity for symmetrical stretching modes of the α -diimine and the carbonyls. Although the involvement of α -diimine vibrations points to the presence of either intraligand or MLCT transitions, intraligand transitions are expected to occur at much higher energy and the low-energy bands will therefore belong to MLCT transitions. The MLCT transitions may originate from the metal–metal bonding orbitals of the cluster or from the $\text{Os}(d_{\pi})$ orbitals of the $\text{Os}-\alpha$ -diimine moiety. The RR effect of $\nu_s(\text{CO})$ excludes the former possibility since the CO-bonds will only be affected by the latter type of transitions. This has been demonstrated for a series of α -diimine ($=\text{L}$) complexes such as $\text{M}(\text{CO})_4(\text{L})$ ($\text{M} = \text{Cr}, \text{Mo}, \text{W}$),^{34,35} $(\text{CO})_5\text{MnRe}(\text{CO})_3(\text{L})$,^{41,42} and $(\text{CO})_5\text{MnRe}(\text{CO})_3(\mu\text{-L})\text{ML}'_n$ ($\text{ML}'_n = \text{Re}(\text{Br})(\text{CO})_3, \text{W}(\text{CO})_4$)⁴¹ or $\text{Ni}(\text{CO})_2(\text{L})$.⁴³ According to the RR spectra of these complexes, depopulation of a metal- d_{π} orbital by MLCT excitation is always accompanied by a RR effect for $\nu_s(\text{CO})$, demonstrating the decrease of metal-to-CO π -back-bonding and concomitant change of CO-bond lengths. This observation is of importance for the mechanism of the photoreaction to be discussed hereafter.

All photochemical experiments show the formation of a transient species, whose lifetime depends on the coordinating ability of the solvent. In toluene the MLCT lifetimes are very

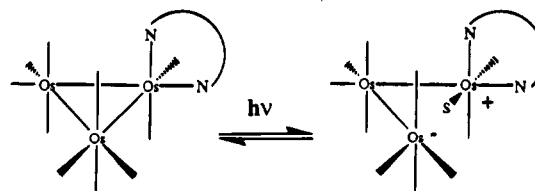


Figure 7. Photochemical reaction of the clusters $\text{Os}_3(\text{CO})_{10}(\text{L})$ in a coordinating solvent (S).

short (<10 ns), much shorter than that observed for the corresponding mononuclear complex $\text{Re}(\text{Cl})(\text{CO})_3(\text{bpy})$ ⁴⁴ (65 ns). Apparently, there is a fast nonradiative decay from the lowest MLCT state when bpy is coordinated to the cluster fragment $\text{Os}_3(\text{CO})_{10}$.

The lifetimes of the transient species are much longer when a coordinating solvent such as THF or acetonitrile is used instead of toluene. In fact, these lifetimes are so long that the transient species cannot be assigned to an excited state anymore but has to be a photoproduct. Thus, in THF the lifetimes vary at room temperature from ca. 200 to 900 ns, depending on the diimine ligand used. The transient species even became a stable photoproduct in this solvent when the photoreaction was performed at 173 K. The influence of the coordinating ability of the solvent was also evident from the photoreactions in acetonitrile and pyridine. In acetonitrile the lifetime varied from 5 to 20 s; in pyridine a lifetime of 20 min was observed for the photoproduct of $\text{Os}_3(\text{CO})_{10}(\text{bpy})$. Finally, a stable photoproduct was obtained when such an $\text{Os}_3(\text{CO})_{10}(\text{L})$ complex was irradiated at room temperature in THF in the presence of excess Bu_4NX ($\text{X} = \text{halide}$). The strong influence of the coordinating ability of the solvent on the stability of the photoproduct clearly demonstrates that this photoproduct has an open site at which the solvent can coordinate.

Coordination of the solvent, $\text{P}(\text{OMe})_3$, or Bu_4NX has also a dramatic influence on the absorption spectra of the photoproduct, as can be seen from Table 5 and Figure 6. In THF at room temperature, coordination of the solvent is weak. It becomes more prominent when the temperature is lowered (2-MeTHF, 133 K), when acetonitrile (pyridine) is used as a solvent, or when $\text{P}(\text{OMe})_3$ or Bu_4NX is added to the solution. This increase of bond strength is accompanied by a large shift of the MLCT band to lower energy due to the strong influence of electron-donation by the solvent, $\text{P}(\text{OMe})_3$, or X^- on the metal- d orbitals. This strong dependence of the MLCT transitions on the solvent coordination also shows that the open site is localized at the $\text{Os}-\alpha$ -diimine moiety.

The photoproduct is not a (di)radical species since it does not show any ESR signal, even in the presence of a radical scavenger such as $t\text{-BuNO}$. Moreover, the photoproduct does show an $^1\text{H-NMR}$ signal with the proton resonances of the α -diimine ligand shifted downfield. The RR and IR spectra of the photoproduct also show that the α -diimine ligand is still coordinated as an uncharged, chelating ligand to Os. Thus, irradiation of these clusters leads to the formation of a photoproduct possessing a coordinatively unsaturated, positively charged, $\text{Os}-\alpha$ -diimine moiety. The photoproduct is therefore proposed to have the zwitterionic structure depicted in Figure 7. This structure fully agrees with the properties of the transients discussed above.

Back-reaction to give the parent cluster is achieved by nucleophilic attack of the negative part of the zwitterion at the cationic $\text{Os}-\alpha$ -diimine moiety. This back-reaction will of course be hampered and may even be prevented when a solvent

(41) van Outersterp, J. W. M.; Stufkens, D. J.; Fraanje, J.; Goubitz, K.; Vlček, A., Jr. *Inorg. Chem.* **1995**, *34*, 4756.

(42) Kokkes, M. W.; Snoeck, T. L.; Stufkens, D. J.; Oskam, A.; Christophersen, M.; Stam, C. H. *J. Mol. Struct.* **1985**, *131*, 11.

(43) Servaas, P. C.; Stufkens, D. J.; Oskam, A. *Inorg. Chem.* **1989**, *28*, 1774.

(44) Kalyanasundaram, K. *J. Chem. Soc., Faraday Trans. 2* **1986**, *82*, 2401.

molecule, a ligand such as P(OMe)_3 , or an anion blocks the open site. This explains the large influence of the coordinating properties of the solvent on the lifetime of the zwitterion. Coordination of a hard base such as THF will be sensitive to the charge donated by the α -diimine. This charge effect decreases when this ligand becomes a stronger π acceptor in the order $\text{bpy} > \text{bpym} > \text{dpp}$.³⁹ In the same order, the metal–solvent bond will be strengthened, and this has a retarding effect on the back-reaction of the zwitterion to the parent complex. As a result, the lifetime of the zwitterion is expected to increase, and this is in accordance with our observations (Table 3).

The question remains how these zwitterions are formed after excitation into the MLCT transitions of the clusters. In this respect the time-resolved absorption spectra are revealing since they show the presence of the zwitterion as a single photoproduct in THF within the time domain 50 ps to 1 μs . This photoproduct merely reacts back to give the parent complex. Thus, the zwitterion is already present within 50 ps after the laser pulse, which means that it is most probably formed directly from the MLCT excited state(s) and not via a diradical or carbonyl bridged intermediate. Such an intermediate would certainly have a much longer lifetime than a few picoseconds.

Since none of the intermediates are formed which have been detected upon photolysis of $\text{Os}_3(\text{CO})_{12}$ (carbonyl bridged isomer)^{11,13} or of metal–metal bonded dinuclear complexes such as $\text{L}_n\text{M}'\text{Re}(\text{CO})_3(\alpha\text{-diimine})$ ($\text{L}_n\text{M}' = (\text{CO})_5\text{Mn}, (\text{CO})_4\text{Co}, \text{Ph}_3\text{-Sn}$, etc.) (radical formation by homolysis of the $\text{M}'\text{-Re}$ bond),^{15–22} the photochemical mechanism of the $\text{Os}_3(\text{CO})_{10}(\text{L})$ complexes must be different.

Irradiation of $\text{Os}_3(\text{CO})_{10}(\text{L})$ into the MLCT transitions leads to a separation of charge in the MLCT states of these complexes. A solvent molecule may attack the positively charged Os atom of the $\text{Os}(\text{CO})_2(\alpha\text{-diimine})$ moiety with formation of a seven coordinated metal center.^{45,46} As a result of the extra negative charge donated by the solvent there will be an unfavorable charge distribution between the $\text{Os}(\text{CO})_2(\text{S})(\alpha\text{-diimine})$ and $\text{Os}(\text{CO})_4$ fragments for metal–metal bond formation. The bonds become more ionic and finally undergo a heterolytic splitting, giving rise to the zwitterion formation. It is clear that such a heterolytic splitting will not occur when the cluster is photolyzed in a noncoordinating solvent such as toluene. In such a solvent the complex will decay to the ground state from the MLCT states. Up to now, light-induced heterolytic splitting of a metal–metal bond has only been reported for the complex $\text{Cp}(\text{CO})_2\text{FeCo}(\text{CO})_4$ in an Ar matrix doped with CO.⁴⁷ In all other cases, in which ionic products were formed photochemically, the photoreactions appeared to proceed via homolytic splitting of a metal–metal bond, followed by coordination of a solvent or reactant and electron transfer.^{16,19} It is, however, well-established that extra negative charge at the α -diimine substituted fragment of a metal–metal bonded complex may induce heterolysis of the metal–metal bond. Thus, electrochemical

reduction of the complexes $(\text{CO})_5\text{MnRe}(\text{CO})_3(\alpha\text{-diimine})$ gives rise to the formation of $\text{Mn}(\text{CO})_5^-$ and a $[\text{Re}(\text{CO})_3(\alpha\text{-diimine})]^+$ radical species.⁴⁸ Besides, if the π accepting α -diimine is replaced by a chelating σ donor ligand such as 1,2-bis-(diphenylphosphino)ethane, no metal–metal bonded complex $(\text{CO})_5\text{MnMn}(\text{CO})_3(1,2\text{-bis}(\text{diphenylphosphino})\text{ethane})$ is formed by reaction of the ions $\text{Mn}(\text{CO})_5^-$ and $^+\text{Mn}(\text{CO})_3(\text{L})(1,2\text{-bis}(\text{diphenylphosphino})\text{ethane})$,⁴⁹ although the reaction between $\text{Mn}(\text{CO})_5^-$ and $^+\text{Mn}(\text{CO})_3(\text{L})(\alpha\text{-diimine})$ proceeds very rapidly.¹⁵ This again illustrates the influence of charge distribution between metal fragments on the stability of the metal–metal bond.

Proof for the correctness of the proposed associative mechanism cannot be given at the moment but may be provided by studying the influence of steric effects of solvents, reactants, and α -diimine ligands on the zwitterion formation and by a pressure dependent quantum yield study. Such experiments are planned and partly in progress.

In contrast to $\text{Os}_3(\text{CO})_{10}(\text{L})$ ($\text{L} = \text{bpy}, \text{bpym}, \text{dpp}$), the complex $\text{Os}_3(\text{CO})_{10}(\text{dpb})$ is not photoreactive. This may be caused by the large decrease of the MLCT state energy (Table 5). Because of this low energy, nonradiative decay to the ground state becomes more important and may compete efficiently with the zwitterion formation. Alternatively, heterolytic splitting of a metal–metal bond with formation of a zwitterion, may be prevented here because of the strong π acceptor properties of the dpb ligand.

Conclusions

A solvent dependent, reversible osmium–osmium bond opening is observed for the compounds $\text{Os}_3(\text{CO})_{10}(\text{L})$ ($\text{L} = \text{bpy}, \text{bpym}, \text{dpp}$), whereas $\text{Os}_3(\text{CO})_{10}(\text{dpb})$ is photostable. The bond opening and closing mechanism proceeds via a zwitterionic intermediate. The zwitterion can also undergo an electrophilic attack by AlCl_3 .

The physical and chemical properties of the solution will strongly be altered by the zwitterion formation. Its color changes and also the dielectric constant will change dramatically. Moreover, the solvated cationic site of the zwitterion may also bind and activate molecules that participate in stoichiometric or catalytic reactions. The practical applications of these effects are the subject of a detailed study.

Acknowledgment. D. K. Sharma (Concordia University, Montreal) is gratefully acknowledged for recording the picosecond absorption spectra. D.J.S. thanks C. H. Langford for his great hospitality during his visit to Montreal. J. Nijhoff is thanked for supplying the $^1\text{H-NMR}$ spectra of the zwitterion in deuterated pyridine. A. Vlcek, Jr., is thanked for critical reading of the manuscript. The Netherlands Foundation for Chemical Research (SON) and the Netherlands Organisation for Pure Research (NWO) are thanked for financial support.

IC9413124

(45) Mann, K. R.; Gray, H. B. *J. Am. Chem. Soc.* **1977**, *99*, 306.

(46) Van Dijk, H. K.; Servaas, P. C.; Stufkens, D. J.; Oskam, A. *Inorg. Chim. Acta* **1985**, *104*, 179.

(47) Fletcher, S. C.; Poliakkoff, M.; Turner, J. J. *J. Organomet. Chem.* **1984**, *268*, 259.

(48) van Outersterp, J. W. M.; Hartl, F.; Stufkens, D. J. *Organometallics* **1995**, *14*, 3303.

(49) Morse, D. L.; Wrighton, M. S. *J. Organomet. Chem.* **1977**, *125*, 71.